Analytical Methods

Accepted Manuscript

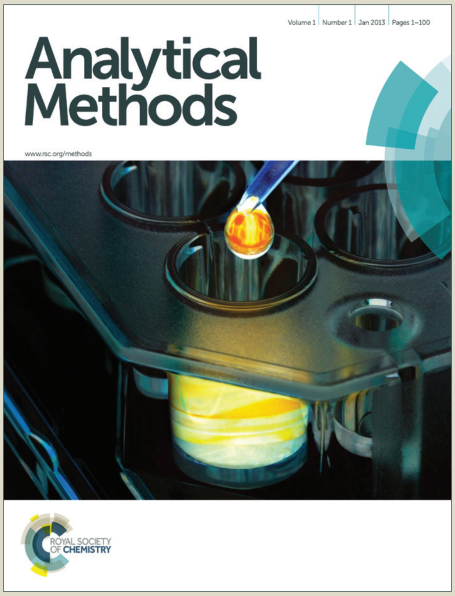

ROYAL SOCIETY OF CHEMISTRY

www.rsc.org/methods

Dynamic Article Links ►

Cite this: DOI: 10.1039/c0xx00000x

www.rsc.org/xxxxxx

ARTICLE TYPE

Analytical study to evaluate the origin and severity of damage caused by salt weathering in a Historical Palace House: The attack of infiltration water

Olivia Gómez-Laserna,*[a] Nagore Prieto-Taboada,[a] Héctor Morillas,[a] Iker Arrizabalaga,[a] Mª Angeles Olazabal,[a] Gorka Arana[a] and Juan Manuel Madariaga[a]

Received (in XXX, XXX) Xth XXXXXXXXX 20XX, Accepted Xth XXXXXXXXX 20XX
DOI: 10.1039/b000000x

The attack of acid infiltration water over a historical building was thoroughly studied by a combination of ion chromatography, chemometric and thermodynamic chemical modelling. The treatment of the quantitative data pointed out to the formation and damage mechanisms of degradation compounds (salts of nitrates, sulphates and chlorides). Apart from that, the values of soluble salts content were evaluated by comparison with current guides, in order to advise the required actions of restoration. Besides, the results revealed that the salts followed the Arnold and Zehnder´s model distribution, by capillarity effect. Using this multianalytical methodology, the principal mechanisms of decay were established.

INTRODUCTION AND OBJECTIVES

The Built Heritage characterizes a society due to its intrinsic value, as an intangible asset. However, the way in which it is preserved could make it a tangible good, as its regeneration and sustainability could generate in return economic benefits in all areas of the society.

During the last decade, the scientific and technical community made significant efforts to preserve the Built Heritage. Nevertheless, the building materials degradation is a natural and irreversible process and before carrying out its maintenance, preservation or revitalization, the causes of deterioration have to be understood. In the same sense, to assure a successful corrective action a deep knowledge of building materials and mechanisms of decay presented is required.

The process of stone decay occurs in different ways. Sometimes it can be gradual, leaving a firm surface. Other times, it can lose its integrity and disintegrate. Even when the material appears to be in perfect conditions, it could have lost its cohesion beneath the surface.

Actually, one of the most harmful effects over construction materials that can be overlooked is caused by soluble salts [1-4]. In the case of buildings located in urban areas, with low levels of air pollution, the most common source of soluble salts is the entrance of runoff and/or subsoil water [5-7]. Its action over building materials can undergo rapid processes such us leaching, transport, accumulation, concentration of solutes, precipitation and local concentration of complex systems of saline solutions, which are transported by capillarity ascension and, ultimately, can precipitate [8-9].

The most damaging salts for building materials are often highly soluble and are easily transported through the porous material by water. In this way, the content inherent to the material can be altered by ions present in water such us nitrates, sulfates and chlorides. At this point, the salts crystallize from a supersaturated solution and their growth within porous materials produces continues local pressures, increasing the size of the empty spaces. Once the critical stress is reached, it is able to overcome the tensile strength of the material.

Furthermore, some salts can take or release hydration water or suffer structural changes, developing new pressures in the pores, which could cause fracture of the material [9-11].

In addition to this, it should be highlighted that the strength of the material depends on a range of variables such as the type of salt to be formed, its properties (solubility changes, thermal expansion coefficient...), its concentration, the degree of supersaturation attained and the petrographic characteristics of the stone (type, distribution voids, water absorption capacity and so on) [12-13]. Hence, the final deterioration is the result of a really complex mechanism and for that reason, before considering any conservation intervention, we have to know the kind of deterioration present.

In this work, we present an analytical methodology to evaluate the real conservation state of materials composing a famous historical Palace House. To achieve this aim the study was carried out in two phases. In a previous work, the molecular composition of degradation products in building materials of the Palace House were identified through the application of in situ analysis by spectroscopic techniques. Then, once confirmed the nature of the soluble salt affection of the building by non destructive methods, in this second phase a multidisciplinary approach was adopted to study the amount and distribution of those affections. Thus, the objective was to find out the origin and mechanism of salt formations, as well as the severity of the damage caused in the different materials of the Palace, as the effectiveness of treatments of conservation, both preventive and active, will depend on them.

For this purpose, the quantification of soluble salts was carried out by ion chromatography, and subsequently, a chemometric analysis of ion content of the materials was also performed. Finally, to clarify the manner in which the salts can damage the walls, thermodynamic models of the different chemical processes that take place in the building were assessed.

EXPERIMENTAL

LOCATION OF THE BUILDING

The Palace is situated in the village of Azpeitia (Gipuzkoa, Basque Country, North of Spain), along the Urola river and, under the limestone Izarraitz massif. Given its proximity to the coast, it has an Atlantic climate with an Oceanic trend (Cfb according to the Köppen-Geiger classification) (Fig. 1). The main economical activities of the town are linked to the primary sector especially, agriculture and livestock. The reports of chemical quality of the Urola water have good levels, although historically, the high rural activity was a problem, causing moderate pollution and certain levels of eutrophy (Grade II and level 69, according to the Iberian Water BioMonitoring Procediment, IBMWP) [14-15].

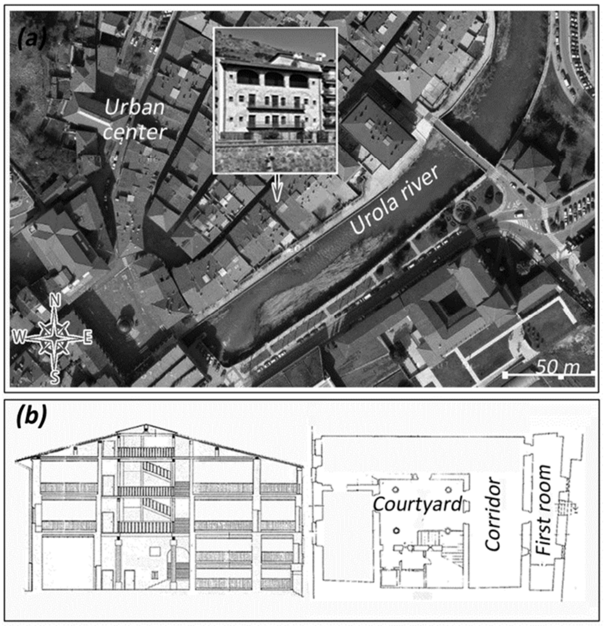

Fig.1 (a) Geographic location of the studied historical building (Basozabal Palace House, Azpeitia, Basque Country, North of Spain), (b) Architectural drawings corresponding to plan and section of the building, where selected sampling areas are indicated on the right hand side.

DESCRIPTION OF THE BUILDING

The building is distributed into ground floor, mezzanine and two upper floors plus an undercover (Fig.1).

The distribution in the ground floor consists of the following: a central courtyard, substantially square with a stairway attached, which allows access to the upper floors. The courtyard is supported on octagonal stone columns of gothic bases and they form a perimeter corridor that allows the passage to the different rooms (Fig. 1).

In 1990 a restoration project was started to use the building as an exhibitions hall but, few years later, the works were suspended and its conservation state is getting worse very rapidly. Only facades, stairway and skylight were rehabilitated.

It is mainly constructed with glauconitic subarkose sandstone and limestone slabs from Igueldo quarry (Donostia, North of Spain) over a concrete base. Sandstones are found in all rooms whereas the limestone is only present in the main facade and in the first room. Nevertheless, in the latter, the ashlars are very small, being sand joint mortar the predominant material. Besides, Portland cement mortar was incorporated in stairway, windows and sills during the restoration.

PRELIMINARY NON-DESTRUCTIVE ANALYSIS

In order to confirm the affection and to justify the sampling of the historical palace, with high cultural relevance, and non destructive in-situ analysis was carried out.

In this way, characteristics and composition of the original material as well as present decaying compounds were identified using mainly Raman spectroscopy. The results, of the stone, corroborated by bibliographic studies [16-18], showed that the detrital components of the sandstone are mostly cemented by carbonate, mainly of sodium and calcium. Besides, the stone contains an important amount of quartz (SiO_2), potassium feldspar ($KAlSi_3O_8$) and iron oxides. The limestone, mainly composed by calcite ($CaCO_3$), contains approximately a 20% of potassium feldspar and carbon. To complete, the sand mortar was composed mainly of calcite, quartz and as minor compound by potassium feldspar [19].

As degradation compounds, a variety of carbonated efflorescence salts were detected such us natrite (Na_2CO_3), termonatrite ($Na_2CO_3{\cdot}H_2O$), natron ($Na_2CO_3{\cdot}10H_2O$), trona ($Na_3(HCO_3)(CO_3){\cdot}2H_2O$) and gaylussite ($Na_2Ca(CO_3)_2{\cdot}5H_2O$), which indicate a transformation of original compounds of sandstone by influence of water. Gypsum ($CaSO_4{\cdot}2H_2O$) and nitratine ($NaNO_3$) were identified as decaying compounds of sandstone, whereas niter (KNO_3) and thenardite (Na_2SO_4) were the most abundant in mortars. According to the results, the existence of these compounds appeared to be related to the presence of infiltration waters, which could increase the salt content of the building materials as well as, encourage their dissolution[19] by the incorporation of new compounds ground leachate or dragged from other materials.

SAMPLING CAMPAIGN

The sampling campaign was performed during the month of February, in accordance to the visual inspection and a preexisting in-situ spectroscopic study taken place previously, following the Italian guidelines (Normal 3/80) [19-20]. The visual inspection allowed the identification of several types of efflorescences, subefflorescences, scalings, flaking and disaggregations as the main affections of the materials in the ground floor wall, which was not restored. Besides, the apparent presence of front salts, up to 1.7 m in height, was observed along the inner wall of the first room (Fig. 2). In this manner, eleven sandstone and mortar samples of the internal walls were gathered, in sufficient amount for analysis of soluble salts, at different range of heights; low (from 0 to 0.2 m), medium and high (0.8 and 1.7 m, respectively) (Table 1).

Fig. 2 Photographs of the deterioration observed in the Palace House; (a) Details of flaking over sandstone of the central courtyard, (b) Sandstone structural column details of the central courtyard, (c) Enlargement of the salts front with an important material loss, in the first instance, (d) Details of efflorescences and subeflorescences over sandstone of the central courtyard.

The samples were collected, trying to damage as little as possible the material, using a chisel and their size was 25x25 mm and 1-3 mm of thickness, approximately.

Prior to the quantitative analysis, the visible efflorescences of the samples were removed in order to quantify the real content of the building materials. Moreover, the removed soluble salts were analyzed too (EM1, EM2, and EM5 samples).

Table 1 Building material samples collected in the Palace House studied. The kind of material, height on the wall and zone of the building is indicated.

Sample	Material	Height	Zone
SM1	Sandstone	Medium	Courtyard
EM1	Subefflorescence	Medium	Courtyard
SM2	Sandstone	Low	Courtyard
EM2	Efflorescence	Medium	Courtyard
SM3	Sandstone	Medium	Courtyard
SM4	Sandstone	Medium	First room
MM5	Mortar	High	First room
EM5	Efflorescence	High	First room
MM6	Mortar	Low	First room
MM7	Mortar	Low	First room
SM8	Mortar	Medium	First room
MM9	Mortar	Low	Corridor
MM10	Mortar	Low	Courtyard
MM11	Mortar	Low	First room

INSTRUMENTS AND METHODS

The methodology selected to carry out the study was performed in two steps. Firstly, to extract the soluble salts of the different building materials, selected samples were milled using agate mortar and were subsequently sieved at 0.1 mm in order to facilitate the extraction. Then, samples were treated in triplicate following an ultrasound assisted extraction method [21], as effective alternative to the standard EN 16455/2014. The extraction was performed in an ultrasound bath, for 120 min using 100 mL of deionised water and 0.1 g of sample by replica. The quantification of content was carried out by a Dionex ICS 2500 suppressed ion chromatography (IC) with a conductivity detector ED50. For the separation of anions, an IonPac AS23 (4x250 mm) column and IonPac AG23 (4x50 mm) precolumn were used. As mobile phase, solutions of 4.5 mM Na_2CO_3/0.8 mM $NaHCO_3$ were selected. The conditions of suppression current and flow applied were 25 mA and 1mL/min, respectively. The quantification of cations was conducted by an IonPac CS12A (4x250 mm) column and IonPac CG-12A (4x50 mm) precolumn from Vertex. As mobile phase, a solution of 20 mM CH_4SO_3 was selected. The suppression current and flow applied were 50mA and 1mL/min, respectively. The data processing was performed by means of the program Chromaleon Version 6.60-SPla software Dionex Corporation (Sunnyvaley, CA, USA).

In the second step, the obtained quantitative data were analysed through a chemometric model. In this manner, The Unscrambler® Version 9.2 software CAMO Process AS (Oslo, Norway) was used to identify correlations between quantified cations and anions. For this purpose, the quantitative data were introduced in units of equivalents/kg, since otherwise there would be no way to take into account the charge of each ion when combined with others. Therefore, the equivalents for each anion and cation were calculated according to the following formules, where *(M)* and *(N)* are the equivalents number of anions and cations, and *(m)* and *(n)* their respective valences:

$$M^{m-} equivalents = m \, x \, mol \, M^{m-} (anions)$$
$$N^{n+} equivalents = n \, x \, mol \, N^{n+} (cations)$$

Furthermore, to explain the formation of the most important decay compounds, thermodynamic models were assessed using chemical equilibrium diagrams and information on stability constants included in the free academic programs HYDRA [22] (Hydrochemical Equilibrium-Constant) and Medusa [23] (Make Equilibrium Diagrams Using Sophisticated Algorithms Version 15, software Royal Institute of Technology (Stockholm, Sweden).

RESULTS AND DISCUSSION

QUANTIFICATION OF SOLUBLE SALTS BY ION CHROMATOGRAPHY

Thanks to suppressed ion cromatography, soluble fluoride, sulphate, nitrite, nitrate, chloride, calcium, sodium, potassium and magnesium concentration were quantified (Table 2). To know if the salt removal is necessary, the total soluble content of the samples was calculated (Table 3) in accordance with the UNI guide and the guide of Salt Attack and Rising Damp [24-25]. Apart from that, the percentage of sulphate, chloride and nitrate of the samples were calculated separately (Table 3) to classify the severity of the damage presented, according to a guide issued by Fraunhofer-IRB [26].

According to the results summarized in Table 2 and 3, a high soluble salt content of the materials was revealed. The samples collected in the courtyard showed as major compounds nitrates and sulphates whereas nitrates were the predominant compounds in the first room. Following the classification of salts levels that are considered potentially hazardous for porous materials [26], only samples MM6 and MM7 showed low or medium levels for these compounds.

Cite this: DOI: 10.1039/c0xx00000x

www.rsc.org/xxxxxx

Table 2 Concentration values in mg Kg^{-1} and method repeatabilities, in RSD %, obtained by ion chromatography.

Sample	Na^+	K^+	NH_4^+	Mg^{2+}	Ca^{+2}	Cl^-	NO_3^-	SO_4^{-2}
SM1	4.10 x 10^{+3}	4.10 x 10^{+3}	<QL	< DL	1.30 x 10^{+4}	3.40 x 10^{+3}	1.60 x 10^{+4}	1.80 x 10^{+4}
EM1	2.20 x 10^{+5}	4.30 x 10^{+3}	<DL	< DL	1.70 x 10^{+3}	2.80 x 10^{+3}	5.90 x 10^{+3}	1.60 x 10^{+3}
SM2	2.10 x 10^{+3}	1.10 x 10^{+3}	<QL	< DL	4.40 x 10^{+3}	2.40 x 10^{+3}	6.60 x 10^{+3}	5.70 x 10^{+3}
EM2	2.80 x 10^{+5}	1.0 x 10^{+3}	< DL	< DL	4.30 x 10^{+2}	2.40 x 10^{+2}	1.50 x 10^{+3}	5.90 x 10^{+2}
SM3	4.40 x 10^{+3}	9.60 x 10^{+2}	< DL	< DL	9.70 x 10^{+4}	6.40 x 10^{+3}	8.0 x 10^{+3}	2.40 x 10^{+5}
SM4	4.90 x 10^{+3}	1.10 x 10^{+3}	<QL	1.80 x 10^{+2}	2.80 x 10^{+3}	7.10 x 10^{+3}	7.90 x 10^{+3}	8.20 x 10^{+2}
MM5	3.20 x 10^{+3}	4.70 x 10^{+3}	<QL	< DL	1.10 x 10^{+4}	4.30 x 10^{+3}	2.20 x 10^{+4}	5.10 x 10^{+3}
EM5	1.50 x 10^{+2}	3.80 x 10^{+5}	< DL	< DL	6.30 x 10^{+2}	< DL	8.10 x 10^{+5}	1.20 x 10^{+3}
MM6	2.50 x 10^{+5}	4.20 x 10^{+3}	< DL	< DL	5.0 x 10^{+2}	1.30 x 10^{+3}	2.40 x 10^{+3}	3.60 x 10^{+3}
MM7	2.10 x 10^{+5}	5.90 x 10^{+2}	< DL	< DL	9.10 x 10^{+2}	1.30 x 10^{+3}	2.70 x 10^{+3}	2.0 x 10^{+3}
SM8	7.50 x 10^{+3}	2.0 x 10^{+3}	<QL	< DL	5.50 x 10^{+3}	1.0 x 10^{+4}	1.20 x 10^{+4}	2.40 x 10^{+3}
MM9	4.90 x 10^{+2}	6.10 x 10^{+2}	<QL	1.50 x 10^{+2}	1.60 x 10^{+3}	4.70 x 10^{+2}	6.10 x 10^{+2}	6.0 x 10^{+3}
MM10	9.50 x 10^{+3}	1.20 x 10^{+4}	<QL	2.27 x 10^{+2}	1.70 x 10^{+4}	1.20 x 10^{+4}	3.30 x 10^{+4}	1.90 x 10^{+4}
MM11	4.10 x 10^{+3}	2.90 x 10^{+3}	<QL	3.50 x 10^{+2}	3.24 x 10^{+4}	6.50 x 10^{+3}	2.80 x 10^{+4}	4.0 x 10^{+4}
RSD (%)	2	7	--	4	4	2	4	3
DL[a]	1.5 x 10^{-1}	1.5 x 10^{-1}	3.2 x 10^{-1}	2.2 x 10^{-1}	1.5 x 10^{-1}	2.3 x 10^{-1}	2.6 x 10^{-2}	1.20
QL[b]	4.8 x 10^{-1}	4.7 x 10^{-1}	1.70	7.4 x 10^{-1}	4.7 x 10^{-1}	5.20	1.3 x 10^{-1}	3.50

[a] DL limit of detection, [b]QL limit quantification

The remaining samples showed severe levels, reaching Extreme Grade (IV) in most cases, which indicate high destruction and hygroscopic moisture.

In samples visibly affected by salts (Fig. 2a, 2b) the total content of salt shows percentages above 35%. However, values less than 35% were found in samples that apparently did not showed efflorescences or visible damage, exceeding the limit of 10% considered as gravely polluted according to the UNI standard [24]. These high percentages, similar to values observed in Venice [24], could be caused by dissolution of the main component, in this case calcite. An acid pH is required for this to happen, which in this case is easily reachable by the acid infiltration water of the area, whose pH values were between 5.7 and 6.4 during the samplings carried out.

In addition, it is noteworthy to mention that, samples of mortar, MM10 and MM11, showed more than 10% of salt content. These sampling points correspond to the bases of the walls without damage. However, the top of the wall showed efflorescences, a front of salts and loss of material (Fig 2c). These samples had, as shown in Table 2 and 3, a high content of nitrate. This salt increased in concentration with the distance to the adjacent river facade; given its distribution and high solubility and mobility, the fact that is found at such low points, suggests saline infiltration water as its main source.

According to the data registered about the water of this region, during the last years, high concentrations of ammonium are observed (Fig.3), probably derived from industry and agricultural activities[14]. Therefore, the ground water that could infiltrate in the building constructed close to the water table is probably rich in nitrates as consequence of the rural activity. Besides, its salt content could be increased by ground leachate or even by dragged from other building materials.

Then, the acid content of the infiltration water, in addition to nitrate anions, can react with the original composition of mortars

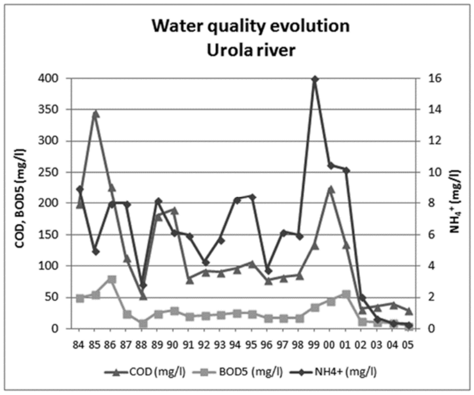

Fig.3 Historic values of ammonium, Chemical and Biochemical oxygen demand (COD and BOD_5, respectively) observed in the Urola River. Information extracted from the report of Gipuzkoa County Council, Department for Sustainable Development, Directorate General of Hydraulic Works [14].

giving rise to the decay compounds [25-27]. The simultaneous presence of ammonium and nitrates, in the same samples (Table 2), suggests that the ammonium nitrate, highly soluble, has not reacted totally. Therefore, it seems that there is a reservoir of this compound coming from the subsoil. Over the years, the walls could have been feeding constantly with salt-bearing moisture, increasing the rising damp caused by capillary action.

In practice, the height to which water will rise in the wall is limited by the rate of evaporation of water from the wall surfaces (related to the masonry materials, surface coatings, climate and so on) [25]. Besides, salt zoning along the wall is the result of fractionating the solution, which depends on the nature of the salt (mobility, solubility, etc...) as well as the above variables. To examine and illustrate the distribution of salt with respect to height in the case under study, the mean values for the ions quantified are shown in Figure 4. A progressive distribution of salt zones was observed. From the first moment, in the rise of water through the wall, the solution starts to evaporate. However, at ground level, the evaporation rate is not enough to effectively concentrate the solution. By contrast, in low and middle areas, the evaporation rate sufficiently exceeds the supply rate of the solution, so that the concentration increases to saturate the less soluble salts, mainly calcium sulphates and sodium carbonates, as Raman spectroscopy also indicated. Once precipitated less soluble salts, the most soluble are available in the solution. Then, to observe efflorescences at highest areas, high values of evaporation rates and mobility are required. In this way, chlorides are located predominantly in the middle region of the wall, and sodium and potassium nitrates at the top. Thus, in low areas, less soluble and mobile salts could be found; in contrast, more soluble and mobile salts migrate towards higher areas. Nevertheless, the amounts of efflorescences observed can be relatively minor, even remain unnoticed, since the precipitation of deliquescent salts depend on the absorption of water from the atmosphere and, they could be condensed, favouring or not its redissolution, as is the case of sodium carbonate. Although, the vertical distribution of salts observed is approximate to Arnold and Zehnder´s model [5,8,28], the salt distribution model can be slightly altered as the acid infiltrated water can increase the concentration of salts by drag from the adjacent original materials[29-30].

Table 3 Values of soluble salt content of the samples (referred to sample weight) obtained by ion chromatography.

Wt %	SO_4^{2-}	Cl^-	NO_3^-	Total salts[a]
SM1	1.8	0.34	1.6	6.9
SM2	0.57	0.24	0.66	2.5
SM3	23.9	0.64	0.80	35.7
SM4	0.08	0.71	0.79	2.8
MM5	0.51	0.43	2.2	6.33
MM6	0.36	0.13	0.24	69.7
MM7	0.20	0.13	0.27	58.2
SM8	0.24	1.0	1.2	4.7
MM9	0.60	0.05	0.06	1.0
MM10	1.9	1.20	3.3	12.2
MM11	4.0	0.65	2.8	14.0

[a] Taking into account bicarbonate content.

Besides, the presence of front salts, located in areas affected by moisture of capillary ascension, under the influence of mortars, seem to point to the idea that its origin is in the saline content of infiltration acid water, which supports the hypothesis again.

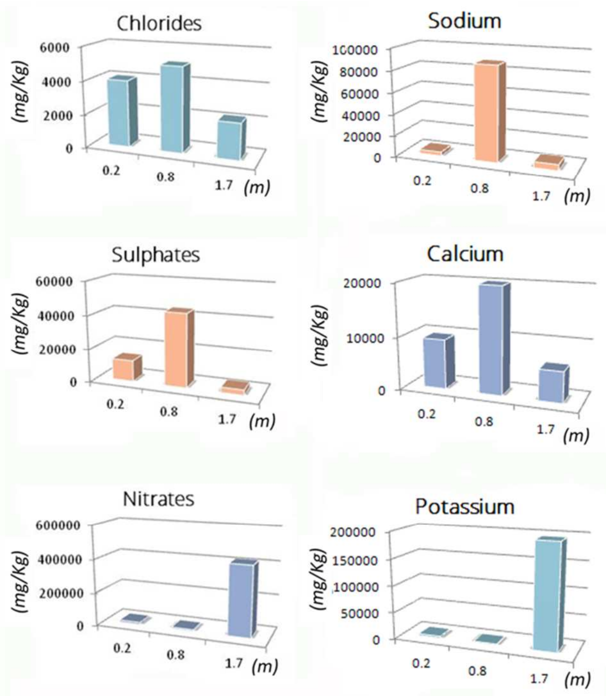

Fig.4 Average of ion content determined by ion chromatography at different heights in the walls at the test site.

PRINCIPAL COMPONENT ANAYLISIS OF THE IC RESULTS

The multivariate analysis of the data was used to obtain further information on the correlation of quantitative analysis. For that purpose, milliequivalents of carbonate were estimated following the equation:

$$\Sigma\ (\text{meq cations}) - \Sigma\ (\text{meq anions}) = \text{meq (carbonate)}$$

Complementary to that estimation, the carbonate content of the samples was correctly checked by an automated system for potentiometric titrations [31] and the Unscrambler results were complemented by correlation analysis of excel software.

The obtained Principal Component Analysis (PCA) explained 87% of the variance, using 3 PCAs to simplify the system. As can be seen in Figure 5, some salts formation is suggested with the grouping of three clusters; sodium and carbonate, potassium and nitrate and magnesium and chloride.

Sodium was extremely correlated with carbonated content (r = 0.999) indicating their common precedence from degradation of the original composition of sandstones. Efflorescence samples EM1 and EM2 were also close to that cluster. This fact is supported with the identification of several carbonated efflorescences in the previous spectroscopic study. These results, together with the entry of acid waters previously shown, demonstrate the damage in the ashlars by loss of original material. In addition to its dissolution and migration, its effect is increased by the equilibrium of hydration of sodium carbonate, which is present in its mono and decahydrated form. As a result, the pressure in the network of pores is increased by the change of volume produced during hydration/dehydration cycles. In fact, natron, the decahydrated form, is ranked as the third most aggressive salt for building materials and, in this case, it is suggested as the main cause of the disintegration and flaking of sandstone [32].

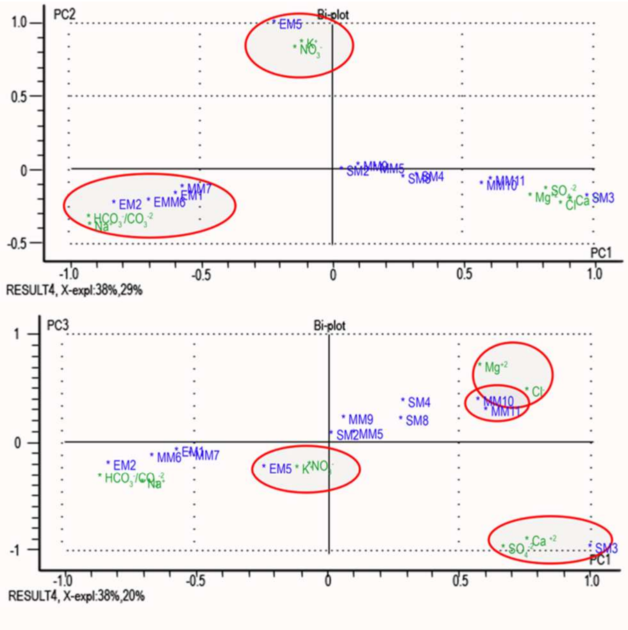

Fig.5 PCAs carried out by Unscrambler . a) Representation of PC1 vs PCA2 of the results obtained by ion chromatographic b) PC1 vs PCA3. Representation of groups formed according to the main three principal components are highlighted: carbonate, nitrates, sulphates and chloride.

Moreover, sodium shows a low negative correlation with chloride (r = -0.470), which could indicate that the source of chloride is not original, confirming, as with its observed levels (Fig 4), it comes with the infiltration water and its passage through the ground.

Potassium is only correlated with nitrate (r = 0.999) and, the proximity of EM5 (Fig 5), efflorescence of the front salt, indicates its main composition. The origin of potassium could be related to two different sources, salt content of the infiltration water and/or it could correspond to an original compound of mortar and limestone. Therefore, this formation mechanism will be studied later in depth.

Apart from that, calcium highly correlates with sulphates (r = 0.981). The formation of calcium sulphates in carbonated materials is a known process. Its formation needs an acid medium to dissolve the original calcite and a sulphate input, which, in this case, could be explained by the action of acid waters over original carbonate, increased by sulphate additives of new mortars and water ion content [29,33-34].

Finally, magnesium is correlated with chlorides, in a lesser extent. Although, in principle this salt is not considered very harmful, studies have demonstrated that the presence of chlorides in solution could encourage dissolution of calcite as well as transformation of the iron oxides [35-37].

The results are quite interesting because the formation of magnesium chloride was not previously detected by Raman spectroscopy in the previous non-destructive screening due to its ionic bond. Besides, others salts such us sodium nitrate and sodium sulphate, which were detected during the screening phase, were not predicted by the chemometric study. This fact is probably due to the great amount of carbonate salts, which could make them unnoticeable, and/or the sampling was performed in a rainier season. Then, changes in weather conditions could have caused its dissolution.

THERMODYNAMIC MODELLING: MECHANISM OF POTASSIUM METASOMATISM AND NITER FORMATION

Thermodynamic chemical modelling was focused on the better understanding of the chemical reactions involved in the formation of the salt front of nitrates. Since, the formation of calcium sulphate has been widely studied [38-39].

Niter formation by action of infiltration water over the limestone wall was predicted with the help of MEDUSA software and the calculations were carried out using the HYDRA database (Fig 6).

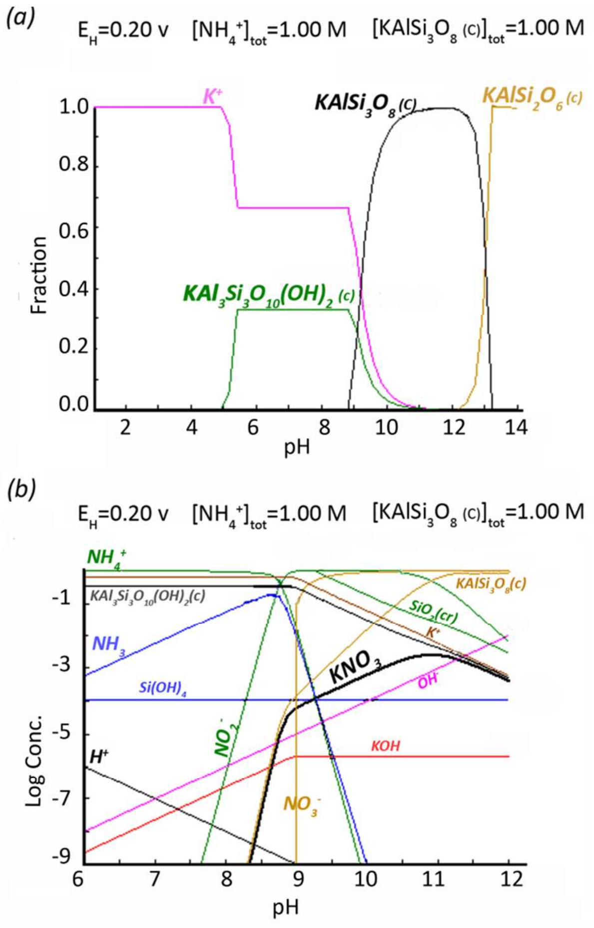

Fig.6 Medusa software chemical prediction of niter formation. Attack mechanism of acid waters over limestone slabs, composed by potassium feldspar and ammonium. Input concentration corresponds to the composition of each material and the historic analyses of water.

According to the discussion of the results, its origin appears to be related to the acid infiltration water action over limestone and mortar materials. Therefore, as source of potassium, the hydrolysis of the aluminum silicate was studied first (Fig 6a). The mass fraction diagram of potassium shows that its hydrolysis starts at pH values lower than 8, which are easily reached by common infiltration waters. In addition, given the presence of a high concentration of ammonium in the waters of this region, the release of potassium is evident (Fig 4).

Subsequently, the action of acid infiltration water content over the feldspar was studied (Fig 6b). Potassium nitrate formation is predicted at pH values higher than 8. These facts suggest the need for its formation in two steps. Firstly, thanks to the low pH of the infiltration waters, leaching of potassium from limestone occurs. It is in the second step, as the calcareous material react (increasing pH) and the drying of materials takes place, when the saturated solution of niter precipitate. Therefore, its formation could be explained by the acid water attack over the original potassium feldspar of limestone and joint mortars. The hydrolysis and the formation of niter seem to follow the reactions 1, 2 and 3.

$$KAlSi_3O_8 + 11H_2O \Leftrightarrow Si_2Al_2O_5(OH)_4 + 4Si(OH)_4 + 2K^+ + 2OH^- \qquad (1)$$

$$KAlSi_3O_{10}(OH)_2 + H^+ + 1.5H_2O \Leftrightarrow 1.5Si_2Al_2O_5(OH)_4 + K^+ \qquad (2)$$

$$K^+ + NO_3^- \Leftrightarrow KNO_3 \qquad (3)$$

Therefore, once the acid water reaches mortar of the wall base, the water content ascends the wall by capillarity effect, hydrolyzing the original compound. The soluble salt reaches the surface and finds a barrier in the limestone, where they crystallize as efflorescences, in joints and surfaces, forming a front of salts, in which niter is the main compound by its high solubility and mobility.

However, although the content of potassium derived from feldspar alteration is particularly high in this kind of materials, and some extra amount from the subsoil is necessary, its presence is probably due to agricultural work in the area too.

CONCLUSIONS

According to the results, the analytical methodology used allows determining the main source of degradation as acid water infiltration from the ground as well as its effect over the original materials. In addition, formation mechanisms of degradation compounds were explained applying chemometric and thermodynamics modelling software. In this manner, the applied methodology points out the importance of understanding the chemistry behind the damage caused by salt weathering over the building materials, as it not only indicates the formation of harmful salts within the materials, but rather it gives an idea of the extent of infiltration water migration in porous systems of masonry materials.

It should be noted that, areas that did not seem visibly affected by soluble salts showed high percentages of soluble salts, evidencing that, in any case, this kind of analytical study is needed not to overlook one of the most harmful pathologies of historic buildings. Likewise, quantitative analysis allowed classifying the degree of the pathology, suggesting necessary desalination process after avoiding or reducing the entrance of water. Moreover, given the loss of material suffered by the transformation of the original compounds and since, some parts such us columns have structural functions, the evaluation about residual hardness of the stones and mortars are suggested to help the conservators to identify a time limit before of a severe damage be caused in the structure. Taking into account the soluble salts values obtained, the consolidation and reinforcement works of the structures are urgent to assure the maintenance of the Palace house.

Finally, as the methodologies based on Raman cannot detect ionic bonds, they must be complemented with other analytical techniques for the detection chlorides, as this compound plays an important role as a catalyst of degradation reactions. Apart from that, the mechanism of niter formation from pH higher than 8 evidence, one more time, the necessity of quantitative analyses to detect its present in humid conditions, as it could be not saturated. Similarly, spectroscopy techniques are really useful to detect damage by hydration and dehydration cycles, as well as by other harmful compounds, as thenardite in this case, as their minor presences could go unnoticed by chemometric studies. Thereby, a combination of both methodologies is really advised to perceive other important sources of degradation, like the effect of additives in materials incorporated into the building during restoration process.

ACKNOWLEDGEMENTS

This work has been financially supported by the project DEMBUMIES from the Spanish Ministry of Economy and Competitiveness (MINECO) (ref:BIA 2011-28148). O. Gómez-Laserna and I. Arrizabalaga are grateful to the University of the Basque Country (UPV-EHU) for their pre-doctoral fellowships. H. Morillas is acknowledged for his grant from the MINECO and the UFI program of the UPV/EHU (ref. UFI 11-26 Global Change and Heritage). Finally, N. Prieto-Taboada is grateful to the University of the Basque Country (UPV/EHU) for her post-doctoral contract.

NOTES AND REFERENCES

[a] *Department of Analytical Chemistry, University of the Basque Country (EHU/UPV), P.O. Box 644, E-48080 Bilbao, Basque Country, Spain. Fax: +34 94 601 35 00; Tel: +34 94 601 82 94; E-mail: olivia.gomez@ehu.es*

1 A. S. Goudie and H. Viles, *Salt weathering hazards*, Wiley, Chichester, UK, 1997.
2 C. R. Navarro, E. Doehne and E. Sebastian, *Cement Concrete Res,* 2000, **30**, 1527-1534.
3 I. Martínez Arkarazo, M. A. Angulo, L. Bartolomé, N. Etxebarria, M. A. Olazabal and J. M. Madariaga, *Anal Chim Acta*, 2007, **584**, 350-359.
4 M. Gómez Heras, B. J. Smith, H. Viles, J. Meneely and S. McCabe, *HD Laser scanning for the evaluation of salt decay laboratory simulations of building limestone*, Proceedings SWBSS, Copenhagen, 2008.
5 E. R. Agudo, B. Lubelli, A. Sawdy, R. V. Hees, C. Price and C. R. Navarro, *Environ Earth Sci,* 2011, **63**, 1475-1486.
6 A. Arizzi and C. Giuseppe, *Environ Earth Sci,* 2014, **71**, 1699-1710.
7 Y. Matsukura, C. T. Oguchi and N. Kuchitsu, *Bull Eng Geol Env,* 2004, **63**, 167-176.

8 M. A. Vázquez, E. Galán, P. Ortiz and R. Ortiz, *Constr Build Mater* 2013, **45**, 95-105.

9 G. W. Scherer, *Cement concrete Res*, 1999, **29**, 1347-1358.

10 J. Aramendia, L. Gómez Nubla, I. Arrizabalaga, N. Prieto Taboada, K. Castro and J. M. Madariaga, *Corros Sci,* 2013, **76**, 154-162.

11 N. Prieto Taboada, I. Ibarrondo, O. Gómez Laserna, I. Martínez Arkarazo, M. A. Olazabal and J. M. Madariaga, *Hazard Mater,* 2013, **248**, 451-460.

12 *American Society for Testing and Materials*, PA ASTM International, West Conshohocken, 1998.

13 C. A. Doehne and C. Price, *Stone Conservation overview of current research*, Getty Conservation Institute, Los Angeles, 2010.

14 Gipuzkoa County Council, *Bases para la elaboración de las directrices sobre el uso sostenible del agua en Gipuzkoa (Study of river quality*), Gipuzkoa County Council, Gipuzkoa, North of Spain, 2006.

15 D. P. Moreno Franco, J. Quintero Manzano and A. Lopez Cuevas, *ContactoS,* 2010, **78**, 25-33.

16 I. Rodríguez-Maribona, M. Zalbide, F. García Garmilla, J.A. Ibáñez and S. Garín, *Constr Mater, 1999, **49**, 19-30.*

17 M. Cano, I. Rodríguez-Maribona, K. Beraza, F. García-Garmilla, I. Yusta, J. A. Ibañez and S. Garín, *Geogaceta, 2001, **30**, 215-218.*

18 E. García-Garmilla, I. Rodríguez-Maribona, M. Cano, M. Zalbide, J. A. Ibañez, E. Osa-Chans and S. Garín, *Constr Mater*, 2002, 52, 5-18.

19 O. Gómez Laserna, M. A. Olazabal, H. Morillas, N. Prieto Taboada, I. Martínez Arkarazo, G. Arana and J. M. Madariaga, *Raman Spectrosc,* 2013, **44**, 1277-1284.

20 C.N.R.-I.C.R, *Materiali Lapidei: Campionamento*, Comas Gráfica, Roma, 1980.

21 N. Prieto Taboada, O. Gómez Laserna, I. Martínez Arkarazo, M. A. Olazabal and J. M. Madariaga, *Ultrasound Sonochem,* 2012, **19**, 1260-1265.

22 N. Ingri, W. Kakolowicz, L. G. Sillén and B. Warnqvist, *Talanta*, 1968, **15**, 1261-1286.

23 I. Puigdomenech, A. Zagorodni, M. Wang and M. Muhammed, *Program Medusa (Make Equilibrium Diagrams Using sophisticated Algoritms*, Royal Institute of Technology, Inorganic Materials Chemistry, Sweden, 2009.

24 E. Pinto, *Risanamento di murate umide e degrádate*, Dario Flaccovio, Italy, 2011.

25 D. Young, *Salt attack and rising damp. A guide to salt damp in historic buildings and older buildings*, Heritage Council of NSW, South Australian, 2008.

26 M. Auras, *Leitfaden Naturstein-Monitoring. Nachkontrolle und Wartung als zukunftsweisende Erhaltungsstrategien*, Stuttgart, Fraunhofer-IRB-Verl, 2011.

27 H. Morillas, M. Maguregui, O. Gómez Laserna, J. Trebolazaba and J. M. Madariaga, *Raman Spectrosc,* 2013, **44**, 1700-1710.

28 M. Auxiliadora Vázquez, E. Galán, M. A. Guerrero and P. Ortiz, *Constr Built Mater*, 2011, **25**, 1603-1611.

29 P. Lopez Arce, E. Doehne, W. Martin and S. Pinchin, *Mater Constr,* 2008, **58**,125-142.

30 C. Hall and D. H. Willian, *Proc R Soc A,* 2007, **463**, 1871-1884.

31 R. Cazallas, L. A. Fernández, N. Etxebarria and J. M. Madariaga, *Lab Robotics Automat,* 1993, **5**, 161.

32 J. G. Talegón and M. A. Vicente, *Mater Construcc*, 1998, **49**, 17-27.

33 M. L. Sánchez de Rojas, N. García and M. Frías, *Mater Construc,* 1998, **49**, 31-41.

34 V. Matović, S. Erić, D. Srećkovic Btoćanin, P. Colomban and A. Kremenović, *Environ Earth Scie,* 2014, **72**, 1939-1951.

35 S. S. Seo, S. M. Son, C. H. Lee and K. Baek, *Compositional analysis of soluble salt in Bresle Extraction from Blocks in Newbuildings Shipyards*, ISST, Osaka, 2007.

36 S. Nikolaos Alexis, P. Theoulakis and C. Pilinis, *Built Environ* , 2009, **44**, 260-270.

37 J. J. McAlister, B. J. Smith and A. Török, *Atmos Environ*, 2006, **40**, 6780-6790.

38 J. Aramendia, L. Gómez Nubla, K. Castro and J. M. Madariaga, *Microchem*, 2014, **115**, 138-145.

39 M. Maguregui, U. Knuutinen, I. Martínez Arkarazo, K. Castro and J. M. Madariaga, *Anal Chem*, 2010, **83**, 3319-3326.

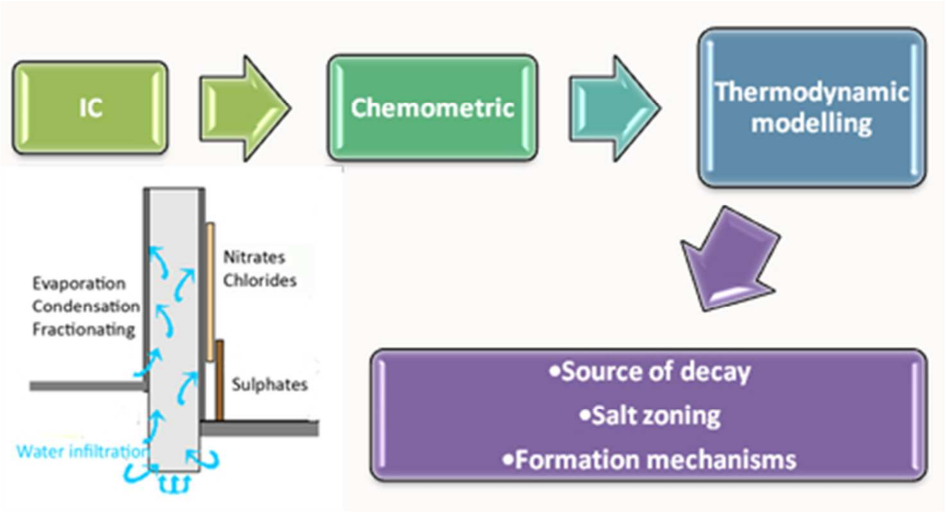

Analytical study to evaluate the origin and severity of damage caused by salt weathering in a Historical Palace House: The attack of infiltration water
79x43mm (150 x 150 DPI)